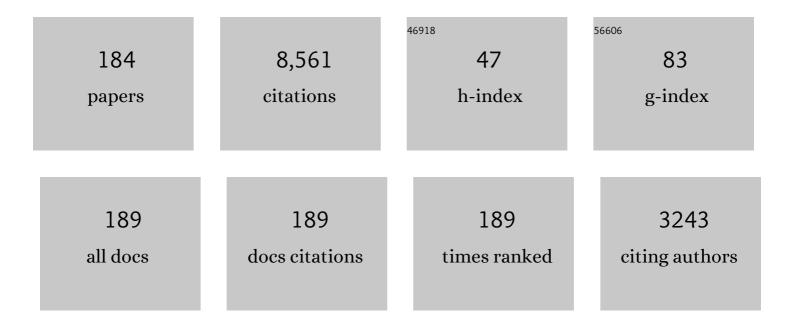
Simon B Duckett

List of Publications by Year in descending order

Source: https://exaly.com/author-pdf/7079729/publications.pdf Version: 2024-02-01



#	Article	IF	CITATIONS
1	Reversible Interactions with para-Hydrogen Enhance NMR Sensitivity by Polarization Transfer. Science, 2009, 323, 1708-1711.	6.0	761
2	lridium N-Heterocyclic Carbene Complexes as Efficient Catalysts for Magnetization Transfer from <i>para</i> -Hydrogen. Journal of the American Chemical Society, 2011, 133, 6134-6137.	6.6	318
3	The theory and practice of hyperpolarization in magnetic resonance using parahydrogen. Progress in Nuclear Magnetic Resonance Spectroscopy, 2012, 67, 1-48.	3.9	317
4	Facing and Overcoming Sensitivity Challenges in Biomolecular NMR Spectroscopy. Angewandte Chemie - International Edition, 2015, 54, 9162-9185.	7.2	258
5	Applications of the parahydrogen phenomenon: A chemical perspective. Progress in Nuclear Magnetic Resonance Spectroscopy, 1999, 34, 71-92.	3.9	222
6	Application of <i>Para</i> hydrogen Induced Polarization Techniques in NMR Spectroscopy and Imaging. Accounts of Chemical Research, 2012, 45, 1247-1257.	7.6	198
7	A theoretical basis for spontaneous polarization transfer in non-hydrogenative <i>para</i> hydrogen-induced polarization. Journal of Chemical Physics, 2009, 131, 194505.	1.2	188
8	Observation of New Intermediates in Hydrogenation Catalyzed by Wilkinson's Catalyst, RhCl(PPh3)3, Using Parahydrogen-Induced Polarization. Journal of the American Chemical Society, 1994, 116, 10548-10556.	6.6	170
9	Spontaneous Transfer of <i>Para</i> hydrogen Derived Spin Order to Pyridine at Low Magnetic Field. Journal of the American Chemical Society, 2009, 131, 13362-13368.	6.6	165
10	A hyperpolarized equilibrium for magnetic resonance. Nature Communications, 2013, 4, 2946.	5.8	126
11	Optimization of SABRE for polarization of the tuberculosis drugs pyrazinamide and isoniazid. Journal of Magnetic Resonance, 2013, 237, 73-78.	1.2	122
12	Parahydrogen-based NMR methods as a mechanistic probe in inorganic chemistry. Coordination Chemistry Reviews, 2008, 252, 2278-2291.	9.5	117
13	Delivering strong ¹ H nuclear hyperpolarization levels and long magnetic lifetimes through signal amplification by reversible exchange. Proceedings of the National Academy of Sciences of the United States of America, 2017, 114, E3188-E3194.	3.3	115
14	Manganese(I)â€Catalyzed Câ^'H Activation: The Key Role of a 7â€Membered Manganacycle in Hâ€Transfer and Reductive Elimination. Angewandte Chemie - International Edition, 2016, 55, 12455-12459.	7.2	111
15	Utilization of SABRE-Derived Hyperpolarization To Detect Low-Concentration Analytes via 1D and 2D NMR Methods. Journal of the American Chemical Society, 2012, 134, 12904-12907.	6.6	110
16	Using <i>para</i> hydrogen to hyperpolarize amines, amides, carboxylic acids, alcohols, phosphates, and carbonates. Science Advances, 2018, 4, eaao6250.	4.7	109
17	Toward Biocompatible Nuclear Hyperpolarization Using Signal Amplification by Reversible Exchange: Quantitative <i>in Situ</i> Spectroscopy and High-Field Imaging. Analytical Chemistry, 2014, 86, 1767-1774.	3.2	105
18	<i>Para</i> -Hydrogen Induced Polarization without Incorporation of <i>Para</i> -Hydrogen into the Analyte. Inorganic Chemistry, 2009, 48, 663-670.	1.9	104

#	Article	IF	CITATIONS
19	Signal Amplification by Reversible Exchange (SABRE): From Discovery to Diagnosis. Angewandte Chemie - International Edition, 2018, 57, 6742-6753.	7.2	101
20	Strategies for the Hyperpolarization of Acetonitrile and Related Ligands by SABRE. Journal of Physical Chemistry B, 2015, 119, 1416-1424.	1.2	87
21	Hyperpolarising Pyruvate through Signal Amplification by Reversible Exchange (SABRE). Angewandte Chemie - International Edition, 2019, 58, 10271-10275.	7.2	87
22	Only para-hydrogen spectroscopy (OPSY), a technique for the selective observation of para-hydrogen enhanced NMR signals. Chemical Communications, 2007, , 1183-1185.	2.2	84
23	Manganese Alkane Complexes: An IR and NMR Spectroscopic Investigation. Journal of the American Chemical Society, 2011, 133, 2303-2310.	6.6	84
24	Hyperpolarisation through reversible interactions with parahydrogen. Catalysis Science and Technology, 2014, 4, 3544-3554.	2.1	84
25	A continuousâ€flow, highâ€throughput, highâ€pressure parahydrogen converter for hyperpolarization in a clinical setting. NMR in Biomedicine, 2013, 26, 124-131.	1.6	83
26	Probing signal amplification by reversible exchange using an NMR flow system. Magnetic Resonance in Chemistry, 2014, 52, 358-369.	1.1	81
27	Exchange Processes in Complexes with Two Ruthenium (η2-Silane) Linkages: Role of the Secondary Interactions between Silicon and Hydrogen Atoms. Organometallics, 2002, 21, 5347-5357.	1.1	75
28	Preparing High Purity Initial States for Nuclear Magnetic Resonance Quantum Computing. Physical Review Letters, 2004, 93, 040501.	2.9	74
29	Para-hydrogen induced polarisation effects in liquid phase hydrogenations catalysed by supported metal nanoparticles. Dalton Transactions, 2009, , 5074.	1.6	73
30	More than INEPT: parahydrogen and INEPT + give unprecedented resonance enhancement to carbon-13 by direct proton polarization transfer. Journal of the American Chemical Society, 1993, 115, 1156-1157.	6.6	72
31	Hydrogen Activation by an Aromatic Triphosphabenzene. Journal of the American Chemical Society, 2014, 136, 13453-13457.	6.6	71
32	Fine-tuning the efficiency of para-hydrogen-induced hyperpolarization by rational N-heterocyclic carbene design. Nature Communications, 2018, 9, 4251.	5.8	71
33	Applications of the parahydrogen phenomenon in inorganic chemistry. Dalton Transactions, 2004, , 2601.	1.6	70
34	Iridium(III) Hydrido N-Heterocyclic Carbene–Phosphine Complexes as Catalysts in Magnetization Transfer Reactions. Inorganic Chemistry, 2013, 52, 13453-13461.	1.9	69
35	Platinum Bis(tricyclohexylphosphine) Silyl Hydride Complexes. Organometallics, 2004, 23, 5744-5756.	1.1	68
36	A Model Iridium Hydroformylation System with the Large Bite Angle Ligand Xantphos:  Reactivity with Parahydrogen and Implications for Hydroformylation Catalysis. Inorganic Chemistry, 2006, 45, 7197-7209.	1.9	67

#	Article	IF	CITATIONS
37	Improving the Hyperpolarization of ³¹ P Nuclei by Synthetic Design. Journal of Physical Chemistry B, 2015, 119, 5020-5027.	1.2	65
38	A para-Hydrogen Investigation of Palladium-Catalyzed Alkyne Hydrogenation. Journal of the American Chemical Society, 2007, 129, 6513-6527.	6.6	60
39	SABRE-Relay: A Versatile Route to Hyperpolarization. Journal of Physical Chemistry Letters, 2018, 9, 1112-1117.	2.1	57
40	The Study of Inorganic Systems by NMR Spectroscopy in Conjunction with Parahydrogenâ€Induced Polarisation. European Journal of Inorganic Chemistry, 2003, 2003, 2901-2912.	1.0	55
41	Manganese(I) atalyzed Câ^'H Activation: The Key Role of a 7â€Membered Manganacycle in Hâ€Transfer and Reductive Elimination. Angewandte Chemie, 2016, 128, 12643-12647.	1.6	54
42	Achieving High Levels of NMRâ€Hyperpolarization in Aqueous Media With Minimal Catalyst Contamination Using SABRE. Chemistry - A European Journal, 2017, 23, 10491-10495.	1.7	54
43	Selective detection of hyperpolarized NMR signals derived from para-hydrogen using the Only Para-hydrogen SpectroscopY (OPSY) approach. Journal of Magnetic Resonance, 2011, 208, 49-57.	1.2	53
44	Direct and indirect hyperpolarisation of amines using <i>para</i> hydrogen. Chemical Science, 2018, 9, 3677-3684.	3.7	53
45	Hyperpolarising Pyruvate through Signal Amplification by Reversible Exchange (SABRE). Angewandte Chemie, 2019, 131, 10377-10381.	1.6	52
46	Long-lived states to sustain SABRE hyperpolarised magnetisation. Physical Chemistry Chemical Physics, 2016, 18, 24905-24911.	1.3	50
47	Observation of H2 oxidative addition to chlorocarbonylbis(triphenylphosphine)rhodium(I) using parahydrogen induced polarization. Journal of the American Chemical Society, 1993, 115, 5292-5293.	6.6	49
48	Utilisation of water soluble iridium catalysts for signal amplification by reversible exchange. Dalton Transactions, 2015, 44, 7870-7880.	1.6	49
49	SABRE hyperpolarization enables high-sensitivity ¹ H and ¹³ C benchtop NMR spectroscopy. Analyst, The, 2018, 143, 3442-3450.	1.7	49
50	Using signal amplification by reversible exchange (SABRE) to hyperpolarise ¹¹⁹ Sn and ²⁹ Si NMR nuclei. Chemical Communications, 2016, 52, 14482-14485.	2.2	48
51	Structure and dynamics in metal phosphine complexes using advanced NMR studies with para-hydrogen induced polarisation. Journal of the Chemical Society Dalton Transactions, 1999, , 1429.	1.1	44
52	Photoinduced N2 loss as a route to long-lived organometallic alkane complexes: A time-resolved IR and NMR study. Chemical Science, 2010, 1, 622.	3.7	44
53	Deactivation of signal amplification by reversible exchange catalysis, progress towards in vivo application. Chemical Communications, 2015, 51, 9857-9859.	2.2	44
54	NMR Studies of Ru3(CO)10(PMe2Ph)2and Ru3(CO)10(PPh3)2and Their H2Addition Products:Â Detection of New Isomers with Complex Dynamic Behavior. Journal of the American Chemical Society, 2001, 123, 9760-9768.	6.6	43

#	Article	IF	CITATIONS
55	Investigating pyridazine and phthalazine exchange in a series of iridium complexes in order to define their role in the catalytic transfer of magnetisation from para-hydrogen. Chemical Science, 2015, 6, 3981-3993.	3.7	43
56	SABRE hyperpolarisation of vitamin B3 as a function of pH. Chemical Science, 2017, 8, 2257-2266.	3.7	43
57	Hydrogenation Studies Involving Halobis(phosphine)–Rhodium(i) Dimers: Use of Parahydrogen Induced Polarisation To Detect Species Present at Low Concentration. Chemistry - A European Journal, 2004, 10, 2459-2474.	1.7	42
58	Definitive Evidence for a Pairwise Addition of Hydrogen to a Platinum Bis(phosphine) Complex Using Parahydrogen-Induced Polarization. Organometallics, 1996, 15, 2863-2865.	1.1	41
59	Direct Comparison of Hydrogenation Catalysis by Intact versus Fragmented Triruthenium Clusters. Angewandte Chemie - International Edition, 2001, 40, 3874-3877.	7.2	41
60	Catalytic Hydrogenation by Triruthenium Clusters: A Mechanistic Study with Parahydrogen-Induced Polarization. Chemistry - A European Journal, 2003, 9, 1045-1061.	1.7	41
61	Optimisation of pyruvate hyperpolarisation using SABRE by tuning the active magnetisation transfer catalyst. Catalysis Science and Technology, 2020, 10, 1343-1355.	2.1	41
62	Ruthenium Dihydride Complexes:Â NMR Studies of Intramolecular Isomerization and Fluxionality Including the Detection of Minor Isomers by Parahydrogen-Induced Polarization. Inorganic Chemistry, 2002, 41, 2960-2970.	1.9	40
63	The reaction of M(CO)3(Ph2PCH2CH2PPh2) (M = Fe, Ru) with parahydrogen: probing the electronic structure of reaction intermediates and the internal rearrangement mechanism for the dihydride products. Dalton Transactions, 2004, , 3218-3224.	1.6	39
64	Detection of Intermediates in Cobalt-Catalyzed Hydroformylation Using para-Hydrogen-Induced Polarization. Journal of the American Chemical Society, 2005, 127, 4994-4995.	6.6	39
65	Photochemical Pump and NMR Probe: Chemically Created NMR Coherence on a Microsecond Time Scale. Journal of the American Chemical Society, 2014, 136, 10124-10131.	6.6	39
66	Computational Studies Explain the Importance of Two Different Substituents on the Chelating Bis(amido) Ligand for Transfer Hydrogenation by Bifunctional Cp*Rh(III) Catalysts. Organometallics, 2014, 33, 3433-3442.	1.1	39
67	Reaction Monitoring Using SABRE-Hyperpolarized Benchtop (1 T) NMR Spectroscopy. Analytical Chemistry, 2019, 91, 6695-6701.	3.2	39
68	Detection of Picomole Amounts of Biological Substrates by <i>para</i> -Hydrogen-Enhanced NMR Methods in Conjunction with a Suitable Receptor Complex. Journal of the American Chemical Society, 2007, 129, 11012-11013.	6.6	38
69	Molecular MRI in the Earth's Magnetic Field Using Continuous Hyperpolarization of a Biomolecule in Water. Journal of Physical Chemistry B, 2016, 120, 5670-5677.	1.2	37
70	Luminescent Iridium(I) Diethyldithiocarbamate Complexes:  Synthesis, Structure, and Reactivity Including Stereoselective Hydrogen Oxidative Addition. Journal of the American Chemical Society, 1997, 119, 7716-7725.	6.6	36
71	A Hyperpolarizable ¹ H Magnetic Resonance Probe for Signal Detection 15â€Minutes after Spin Polarization Storage. Angewandte Chemie - International Edition, 2016, 55, 15642-15645.	7.2	36
72	Achieving Biocompatible SABRE: An in vitro Cytotoxicity Study. ChemMedChem, 2018, 13, 352-359.	1.6	36

#	Article	IF	CITATIONS
73	A Simple Route to Strong Carbonâ€13 NMR Signals Detectable for Several Minutes. Chemistry - A European Journal, 2017, 23, 10496-10500.	1.7	34
74	Direct enhancement of nitrogen-15 targets at high-field by fast ADAPT-SABRE. Journal of Magnetic Resonance, 2017, 285, 55-60.	1.2	34
75	Extending the Scope of ¹⁹ F Hyperpolarization through Signal Amplification by Reversible Exchange in MRI and NMR Spectroscopy. ChemistryOpen, 2018, 7, 97-105.	0.9	34
76	Parahydrogenâ€Induced Polarization of Amino Acids. Angewandte Chemie - International Edition, 2021, 60, 23496-23507.	7.2	34
77	Palladium-Catalyzed Hydrogenation:Â Detection of Palladium Hydrides. A Joint Study Using Para-Hydrogen-Enhanced NMR Spectroscopy and Density Functional Theory. Journal of the American Chemical Society, 2006, 128, 9596-9597.	6.6	33
78	Remarkable Levels of ¹⁵ N Polarization Delivered through SABRE into Unlabeled Pyridine, Pyrazine, or Metronidazole Enable Single Scan NMR Quantification at the mM Level. Journal of Physical Chemistry B, 2020, 124, 4573-4580.	1.2	33
79	New perspectives in hydroformylation : a para-hydrogen study. Chemical Communications, 2004, , 1826-1827.	2.2	32
80	Observation of New Intermediates in the Reaction of Dihydrogen with Iridium, Rhodium, and Mixed Metal A-Frame Complexes with Parahydrogen-Induced Polarization. Organometallics, 2000, 19, 2985-2993.	1.1	31
81	A combined parahydrogen and theoretical study of H2 activation by 16-electron d8 ruthenium(0) complexes and their subsequent catalytic behaviour. Dalton Transactions, 2004, , 3616.	1.6	31
82	Generation and interrogation of a pure nuclear spin state by parahydrogen-enhanced NMR spectroscopy: a defined initial state for quantum computation. Magnetic Resonance in Chemistry, 2005, 43, 200-208.	1.1	31
83	Quantification of hyperpolarisation efficiency in SABRE and SABRE-Relay enhanced NMR spectroscopy. Physical Chemistry Chemical Physics, 2018, 20, 26362-26371.	1.3	31
84	The reaction of an iridium PNP complex with parahydrogen facilitates polarisation transfer without chemical change. Dalton Transactions, 2015, 44, 1077-1083.	1.6	30
85	The use of yttrium in medical imaging and therapy: historical background and future perspectives. Chemical Society Reviews, 2020, 49, 6169-6185.	18.7	30
86	An NMR study of cobalt-catalyzed hydroformylation using para-hydrogen induced polarisation. Dalton Transactions, 2009, , 2496.	1.6	29
87	Dalton communications. Rapid characterisation of rhodium dihydrides by nuclear magnetic resonance spectroscopy using indirect two-dimensional methods and para-hydrogen. Journal of the Chemical Society Dalton Transactions, 1995, , 3427.	1.1	28
88	Detection of Ïf-alkane complexes of manganese by NMR and IR spectroscopy in solution: (η ⁵ -C ₅ H ₅)Mn(CO) ₂ (ethane) and (η ⁵ -C ₅ H ₅)Mn(CO) ₂ (isopentane). Chemical Science, 2015, 6, 418-424.	3.7	28
89	Harnessing polarisation transfer to indazole and imidazole through signal amplification by reversible exchange to improve their NMR detectability. Magnetic Resonance in Chemistry, 2017, 55, 944-957.	1.1	28
90	A systematic approach to the generation of long-lived metal alkane complexes: combined IR and NMR study of (Tp)Re(CO)2(cyclopentane). Chemical Communications, 2009, , 1401.	2.2	27

6

#	Article	IF	CITATIONS
91	Relayed hyperpolarization from <i>para</i> -hydrogen improves the NMR detectability of alcohols. Chemical Science, 2019, 10, 7709-7717.	3.7	27
92	Parahydrogenâ€Induced Hyperpolarization of Gases. Angewandte Chemie - International Edition, 2020, 59, 17788-17797.	7.2	27
93	NMR characterisation of unstable solvent and dihydride complexes generated at low temperature by in-situ UV irradiation. Chemical Communications, 2002, , 2836-2837.	2.2	26
94	Detection and Reactivity of Pd((C8H14)PCH2CH2P(C8H14))(CHPhCH2Ph)(H) as Determined by Parahydrogen-Enhanced NMR Spectroscopy. Journal of the American Chemical Society, 2004, 126, 16708-16709.	6.6	26
95	Coordination Chemistry and Diphenylacetylene Hydrogenation Catalysis of Planar Chiral Ferrocenylphosphane-Thioether Ligands with Cyclooctadieneiridium(I). European Journal of Inorganic Chemistry, 2006, 2006, 1803-1816.	1.0	26
96	Rapid ¹³ C NMR hyperpolarization delivered from <i>para</i> -hydrogen enables the low concentration detection and quantification of sugars. Chemical Science, 2019, 10, 10607-10619.	3.7	26
97	Implementation of NMR quantum computation with parahydrogen-derived high-purity quantum states. Physical Review A, 2004, 70, .	1.0	25
98	Dipyridylketone binding and subsequent C–C bond insertion reactions at cyclopentadienylrhodium. Chemical Communications, 2003, , 2332-2333.	2.2	24
99	Creating a hyperpolarised pseudo singlet state through polarisation transfer from parahydrogen under SABRE. Chemical Communications, 2016, 52, 7842-7845.	2.2	24
100	Unlocking a Diazirine Long-Lived Nuclear Singlet State via Photochemistry: NMR Detection and Lifetime of an Unstabilized Diazo-Compound. Journal of the American Chemical Society, 2018, 140, 16855-16864.	6.6	24
101	Characterisation and kinetic behaviour of H2Rh(PPh3)2(μ-Cl)2Rh(PPh3)(alkene) and related binuclear complexes detected during hydrogenation studies involving parahydrogen induced polarisation. Chemical Communications, 2000, , 685-686.	2.2	23
102	A DFT Study on the Mechanism of Palladium-Catalyzed Alkyne Hydrogenation: Neutral versus Cationic Pathways. Organometallics, 2008, 27, 43-52.	1.1	23
103	Catalytic Transfer of Magnetism Using a Neutral Iridium Phenoxide Complex. Organometallics, 2015, 34, 2997-3006.	1.1	23
104	New products in an old reaction: isomeric products from H2 addition to Vaska's complex and its analogues. Chemical Communications, 1999, , 1717-1718.	2.2	22
105	Harnessing asymmetric N-heterocyclic carbene ligands to optimise SABRE hyperpolarisation. Catalysis Science and Technology, 2018, 8, 4925-4933.	2.1	22
106	NMR studies on ligand exchange at [IrH2Cl(CO)(PPh3)2] and [IrH2Cl(PPh3)3] by para-hydrogen induced polarisation. Chemical Communications, 1996, , 2395.	2.2	21
107	New insights into catalytic hydrogenation by phosphido-substituted triruthenium clusters: confirmation of intact cluster catalysis by parahydrogen NMR. Dalton Transactions, 2004, , 2108-2114.	1.6	21
108	Photochemical-mediated solid-state [2+2]-cycloaddition reactions of an unsymmetrical dibenzylidene acetone (monothiophos-dba). CrystEngComm, 2012, 14, 5564.	1.3	21

#	Article	IF	CITATIONS
109	SignalverstÃ ¤ kung durch reversiblen Austausch (SABRE): von der Entdeckung zur diagnostischen Anwendung. Angewandte Chemie, 2018, 130, 6854-6866.	1.6	21
110	Equilibria between isomers of ruthenium dihydride complexes: detection of minor isomers by parahydrogen induced polarisation. Chemical Communications, 1996, , 383.	2.2	20
111	Photochemical Isomerization of N-Heterocyclic Carbene Ruthenium Hydride Complexes:Â In situ Photolysis, Parahydrogen, and Computational Studies. Journal of the American Chemical Society, 2006, 128, 7452-7453.	6.6	20
112	Palladium catalysed alkyne hydrogenation and oligomerisation: a parahydrogen based NMR investigation. Dalton Transactions, 2008, , 4270.	1.6	20
113	A parahydrogen based NMR study of Pt catalysed alkyne hydrogenation. Dalton Transactions, 2010, 39, 3495.	1.6	20
114	Using coligands to gain mechanistic insight into iridium complexes hyperpolarized with <i>para</i> -hydrogen. Chemical Science, 2019, 10, 5235-5245.	3.7	20
115	Activation of H2 by halogenocarbonylbis(phosphine)rhodium(I) complexes. The use of parahydrogen induced polarisation to detect species present at low concentration. Journal of the Chemical Society Dalton Transactions, 1999, , 3949-3960.	1.1	19
116	NMR detection of thermal and photochemical dihydrogen addition products of mono- and tri-nuclear ruthenium complexes containing carbonyl and triphenylphosphine ligands through para-hydrogen induced polarisation. Chemical Communications, 1999, , 1223-1224.	2.2	19
117	Nucleophilic attack on η3-allyl and η2-tetrahydroborate complexes of ruthenium(ii). Dalton Transactions, 2003, , 2603-2614.	1.6	19
118	Achieving High ¹ H Nuclear Hyperpolarization Levels with Long Lifetimes in a Range of Tuberculosis Drug Scaffolds. Chemistry - A European Journal, 2017, 23, 16990-16997.	1.7	18
119	A simple handâ€held magnet array for efficient and reproducible <scp>SABRE</scp> hyperpolarisation using manual sample shaking. Magnetic Resonance in Chemistry, 2018, 56, 641-650.	1.1	18
120	Mechanistic insight into novel sulfoxide containing SABRE polarisation transfer catalysts. Dalton Transactions, 2019, 48, 15198-15206.	1.6	18
121	Parahydrogen enhanced NMR studies on thermally and photochemically generated products from [IrH3(CO)(PPh3)2]. Chemical Communications, 1998, , 923-924.	2.2	17
122	Parahydrogen studies of H2addition to Ir(i) complexes containing chiral phosphine–thioether ligands: implications for catalysis. Dalton Transactions, 2006, , 3350-3359.	1.6	17
123	lridium <i>α</i> arboxyimine Complexes Hyperpolarized with <i>para</i> â€Hydrogen Exist in Nuclear Singlet States before Conversion into Iridium Carbonates. ChemPhysChem, 2019, 20, 241-245.	1.0	17
124	Bridging the Gap from Mononuclear Pd ^{II} Precatalysts to Pd Nanoparticles: Identification of Intermediate Linear [Pd ₃ (XPh ₃) ₄] ²⁺ Clusters as Catalytic Species for Suzuki–Miyaura Couplings (X = P, As). Organometallics, 2021, 40, 3560-3570.	1.1	17
125	Activation of H2 by halocarbonyl bis-phosphine and bis-arsine iridium(i) complexes. The use of parahydrogen induced polarisation to detect species present at low concentration and investigate their reactivityBased on the presentation given at Dalton Discussion No. 4, 10–13th January 2002, Kloster Banz, Germany, Dalton Transactions RSC, 2002, 743-751.	2.3	16
126	Contrasting photochemical and thermal reactivity of Ru(CO)2(PPh3)(dppe) towards hydrogen rationalised by parahydrogen NMR and DFT studies. Dalton Transactions, 2006, , 2072.	1.6	16

#	Article	IF	CITATIONS
127	Improving NMR and MRI Sensitivity with Parahydrogen. Topics in Current Chemistry, 2012, 338, 75-103.	4.0	16
128	Photochemical pump and NMR probe to monitor the formation and kinetics of hyperpolarized metal dihydrides. Chemical Science, 2016, 7, 7087-7093.	3.7	16
129	A Hyperpolarizable ¹ H Magnetic Resonance Probe for Signal Detection 15â€Minutes after Spin Polarization Storage. Angewandte Chemie, 2016, 128, 15871-15874.	1.6	16
130	Reversible photo-isomerization of <i>cis</i> -[Pd(L-i [®] <i>S</i> , <i>O</i>) ₂] (HL =) Tj ETQq0 0 0 rgBT /(<i>trans</i> -[Pd(L-i [®] <i>S</i> , <i>O</i>) ₂] and the unprecedented formation of <i>trans</i> -[Pd(L-i [®] <i>S</i> , <i>N</i>) ₂] in solution. Dalton Transactions, 2019, 48,	Jverlock 1 1.6	16
131	17241-17251. Parahydrogen derived illumination of pyridine based coordination products obtained from reactions involving rhodium phosphine complexes. Dalton Transactions, 2005, , 3773.	1.6	15
132	Using SABRE Hyperpolarized ¹³ C NMR Spectroscopy to Interrogate Organic Transformations of Pyruvate. Analytical Chemistry, 2020, 92, 9095-9103.	3.2	15
133	Diastereoselective Oxidative Addition of Dihydrogen to IrI(CO)((R)-BINAP) and [Ir(CO)2((R)-BINAP)][SbF6]. Inorganic Chemistry, 2007, 46, 1196-1204.	1.9	14
134	Iridium Cyclooctene Complex That Forms a Hyperpolarization Transfer Catalyst before Converting to a Binuclear C–H Bond Activation Product Responsible for Hydrogen Isotope Exchange. Inorganic Chemistry, 2016, 55, 11639-11643.	1.9	14
135	Zintl cluster supported low coordinate Rh(<scp>i</scp>) centers for catalytic H/D exchange between H ₂ and D ₂ . Chemical Science, 2022, 13, 7626-7633.	3.7	14
136	Activation of H2by chlorocarbonylbis(trimethylphosphine)rhodium(I) labilizes CO and produces the new binuclear complex H(Cl)Rh(PMe3)2(Âμ-H)(Âμ-Cl)RH(PMe3)(CO). Journal of the Chemical Society Chemical Communications, 1993, , 1185-1187.	2.0	13
137	Low temperature in situ UV irradiation of [(η5-C5H5)Co(C2H4)2] in the NMR probe: formation of Co(iii) silyl hydride complexes. Dalton Transactions, 2007, , 2993-2996.	1.6	13
138	Photochemical studies of (η ⁵ -C ₅ H ₅)Ru(PPh ₃) ₂ Cl and (η ⁵ -C ₅ H ₅)Ru(PPh ₃) ₂ Me: formation of Si–H and C–H bond activation products. Dalton Transactions, 2014, 43, 1162-1171.	1.6	13
139	Using ² H labelling to improve the NMR detectability of pyridine and its derivatives by SABRE. Magnetic Resonance in Chemistry, 2018, 56, 663-671.	1.1	13
140	Pharmacokinetics of the SABRE agent 4,6-d2-nicotinamide and also nicotinamide in rats following oral and intravenous administration. European Journal of Pharmaceutical Sciences, 2019, 135, 32-37.	1.9	13
141	Kinetic and mechanistic examination of NBu4[IrH2(CO)2I2] and NBu4[RhH2(CO)2I2] via para-hydrogen enhanced NMR spectroscopy. Chemical Communications, 1999, , 889-890.	2.2	12
142	The Detection and Reactivity of Silanols and Silanes Using Hyperpolarized 29 Si Nuclear Magnetic Resonance. Angewandte Chemie - International Edition, 2020, 59, 2710-2714.	7.2	12
143	Reaction of iodocarbonylbis(trimethylphosphine)rhodium(I) with parahydrogen leads to the observation of five characterisable H2 addition products. Journal of the Chemical Society Dalton Transactions, 1998, , 3363-3366.	1.1	11
144	A Parahydrogen Study of Catalytic Hydrogenation by Diphosphane-Substituted Triruthenium Clusters. European Journal of Inorganic Chemistry, 2004, 2004, 4381-4387.	1.0	11

#	Article	IF	CITATIONS
145	Use of the tetrahydroborate ligand as "gate-keeper―and protected hydride ligand: preparation and study of alkyl hydride and acyl hydride complexes of ruthenium(ii). Dalton Transactions, 2006, , 2661-2670.	1.6	11
146	Solvent responsive catalyst improves NMR sensitivity via efficient magnetisation transfer. Chemical Communications, 2016, 52, 8467-8470.	2.2	11
147	Synthesis and hyperpolarisation of eNOS substrates for quantification of NO production by 1 H NMR spectroscopy. Bioorganic and Medicinal Chemistry, 2017, 25, 2730-2742.	1.4	11
148	η ² -Alkene Complexes of [Rh(PONOP- ⁱ Pr)(L)] ⁺ Cations (L = COD, NBD,) Tj [Rh(PONOP- ⁱ Pr)(η-H ₂)] ⁺ . Inorganic Chemistry, 2021, 60, 13903-13912.	ETQq0 0 0 1.9	rgBT /Overl 11
149	Roles of a tetrahydroborate ligand in a facile route to ruthenium(ii) ethyl hydride complexes, and a kinetic study of ethane reductive elimination. Dalton Transactions, 2004, , 3788-3797.	1.6	10
150	Direct reaction of photogenerated diarylcarbenes at square-planar rhodium(i). Dalton Transactions, 2004, , 2746-2749.	1.6	10
151	Characterisation of tri-ruthenium dihydride complexes through the computation of NMR parameters. Dalton Transactions, 2012, 41, 4618.	1.6	10
152	Coherent evolution of para hydrogen induced polarisation using laser pump, NMR probe spectroscopy: Theoretical framework and experimental observation. Journal of Magnetic Resonance, 2017, 278, 25-38.	1.2	10
153	Using hyperpolarised NMR and DFT to rationalise the unexpected hydrogenation of quinazoline to 3,4-dihydroquinazoline. Chemical Communications, 2018, 54, 10375-10378.	2.2	10
154	Reversible Hyperpolarization of Ketoisocaproate Using Sulfoxideâ€containing Polarization Transfer Catalysts. ChemPhysChem, 2021, 22, 13-17.	1.0	10
155	Hyperpolarisation of weakly binding N-heterocycles using signal amplification by reversible exchange. Chemical Science, 2021, 12, 5910-5917.	3.7	10
156	Real-Time High-Sensitivity Reaction Monitoring of Important Nitrogen-Cycle Synthons by ¹⁵ N Hyperpolarized Nuclear Magnetic Resonance. Journal of the American Chemical Society, 2022, 144, 8756-8769.	6.6	10
157	Photochemical reactions of [CH2(î·5-C5H4)2][Rh(C2H4)2]2with silanes: evidence for Si–C and C–H activation pathways. Dalton Transactions, 2005, , 744-759.	1.6	9
158	Activation of a (cyclooctadiene) rhodium(i) complex supported by a chiral ferrocenyl phosphine thioether ligand for hydrogenation catalysis: a combined parahydrogen NMR and DFT study. Dalton Transactions, 2013, 42, 11720.	1.6	9
159	Following palladium catalyzed methoxycarbonylation by hyperpolarized NMR spectroscopy: a parahydrogen based investigation. Catalysis Science and Technology, 2017, 7, 2101-2109.	2.1	9
160	Understanding substrate substituent effects to improve catalytic efficiency in the SABRE hyperpolarisation process. Catalysis Science and Technology, 2019, 9, 3914-3922.	2.1	9
161	Probing the Hydrogenation of Vinyl Sulfoxides Using <i>para</i> -Hydrogen. Organometallics, 2019, 38, 4377-4382.	1.1	9
162	Catalystâ€Substrate Effects on Biocompatible SABRE Hyperpolarization. ChemPhysChem, 2019, 20, 285-294.	1.0	9

#	Article	IF	CITATIONS
163	The Detection and Reactivity of Silanols and Silanes Using Hyperpolarized 29 Si Nuclear Magnetic Resonance. Angewandte Chemie, 2020, 132, 2732-2736.	1.6	9
164	A simple and cost-efficient technique to generate hyperpolarized long-lived 15N-15N nuclear spin order in a diazine by signal amplification by reversible exchange. Journal of Chemical Physics, 2020, 152, 014201.	1.2	9
165	Detection of platinum dihydride bisphosphine complexes and studies of their reactivity through para-hydrogen-enhanced NMR methods. Magnetic Resonance in Chemistry, 2008, 46, S107-S114.	1.1	8
166	Detection of Unusual Reaction Intermediates during the Conversion of W(N ₂) ₂ (dppe) ₂ to W(H) ₄ (dppe) ₂ and of H ₂ O into H ₂ . Journal of the American Chemical Society, 2012, 134, 18257-18265.	6.6	8
167	Competing Pathways in the Photochemistry of Ru(H) ₂ (CO)(PPh ₃) ₃ . Organometallics, 2018, 37, 855-868.	1.1	8
168	In Situ SABRE Hyperpolarization with Earth's Field NMR Detection. Molecules, 2019, 24, 4126.	1.7	8
169	Using <i>para</i> hydrogen induced polarization to study steps in the hydroformylation reaction. Dalton Transactions, 2019, 48, 2664-2675.	1.6	7
170	Addition of H2 to a cationic iridium(I) complex: a study using parahydrogen NMR. Dalton Transactions RSC, 2000, , 2251-2253.	2.3	6
171	Quantitative In Situ Monitoring of Parahydrogen Fraction Using Raman Spectroscopy. Applied Spectroscopy, 2018, 73, 000370281879864.	1.2	6
172	Understanding the mechanism of cis–trans isomerism in photo-active palladium(II) complexes derived from the N,N-di-substituted benzoylthioureas. Inorganica Chimica Acta, 2020, 512, 119884.	1.2	6
173	A role for low concentration reaction intermediates in the signal amplification by reversible exchange process revealed by theory and experiment. Physical Chemistry Chemical Physics, 2020, 22, 5033-5037.	1.3	6
174	Steric and electronic effects on the ¹ H hyperpolarisation of substituted pyridazines by signal amplification by reversible exchange. Magnetic Resonance in Chemistry, 2021, 59, 1187-1198.	1.1	4
175	Separation and characterisation of products of the reaction between propionamide and formaldehyde. Chromatographia, 2002, 55, 307-316.	0.7	2
176	Parawasserstoffâ€induzierte Polarisation von AminosÃ ¤ ren. Angewandte Chemie, 2021, 133, 23688.	1.6	2
177	Exploring the hyperpolarisation of EGTA-based ligands using SABRE. Dalton Transactions, 2021, 50, 2448-2461.	1.6	2
178	Contrasting Photochemical and Thermal Catalysis by Ruthenium Arsine Complexes Revealed by Parahydrogen Enhanced NMR Spectroscopy. European Journal of Inorganic Chemistry, 2022, 2022, .	1.0	2
179	SABRE hyperpolarized anticancer agents for use in ¹ H MRI. Magnetic Resonance in Medicine, 2022, , .	1.9	2
180	Towards measuring reactivity on micro-to-millisecond timescales with laser pump, NMR probe spectroscopy. Faraday Discussions, 2019, 220, 28-44.	1.6	1

#	Article	IF	CITATIONS
181	Parawasserstoffâ€induzierte Hyperpolarisation von Gasen. Angewandte Chemie, 2020, 132, 17940-17949.	1.6	1
182	Frontispiece: Achieving High Levels of NMRâ€Hyperpolarization in Aqueous Media With Minimal Catalyst Contamination Using SABRE. Chemistry - A European Journal, 2017, 23, .	1.7	0
183	Frontispiece: Achieving High ¹ H Nuclear Hyperpolarization Levels with Long Lifetimes in a Range of Tuberculosis Drug Scaffolds. Chemistry - A European Journal, 2017, 23, .	1.7	0
184	Breaking bonds over many timescales: in celebration of Robin Perutz's 70th birthday. Dalton Transactions, 2020, 49, 254-255.	1.6	0